AGU PUBLICATIONS

Geophysical Research Letters

RESEARCH LETTER
10.1002/2016GL069084

Yu He, Yang Sun, and Xia Lu contributed equally to this work.

Key Points:
- The first report of fast K^+ migration in the channel structure of $KAlSi_3O_8$ hollandite
- One-dimensional fast K^+ migration in $KAlSi_3O_8$ hollandite leads to a high and anisotropic ionic conductivity
- The conductivity of $KAlSi_3O_8$ hollandite explains high conductivity anomalies related to subduction zones

Supporting Information:
- Supporting Information S1

Correspondence to:
H. Li,
liheping@vip.gyig.ac.cn

Citation:
He, Y., Y. Sun, X. Lu, J. Gao, H. Li, and H. Li (2016), First-principles prediction of fast migration channels of potassium ions in $KAlSi_3O_8$ hollandite: Implications for high conductivity anomalies in subduction zones, *Geophys. Res. Lett.*, *43*, 6228–6233, doi:10.1002/2016GL069084.

Received 10 APR 2016
Accepted 7 JUN 2016
Accepted article online 8 JUN 2016
Published online 27 JUN 2016

First-principles prediction of fast migration channels of potassium ions in $KAlSi_3O_8$ hollandite: Implications for high conductivity anomalies in subduction zones

Yu He[1], Yang Sun[2], Xia Lu[3], Jian Gao[2], Hong Li[2], and Heping Li[1]

[1]Key Laboratory of High-Temperature and High-Pressure Study of the Earth's Interior, Institute of Geochemistry, Chinese Academy of Sciences, Guiyang, China, [2]Beijing National Laboratory for Condensed Matter Physics, Institute of Physics, Chinese Academy of Sciences, Beijing, China, [3]Department of Mining and Materials Engineering, McGill University, Montreal, Quebec, Canada

Abstract Materials sharing the hollandite structure were widely reported as fast ionic conductors. However, the ionic conductivity of $KAlSi_3O_8$ hollandite (K-hollandite), which can be formed during the subduction process, has not been investigated so far. Here first-principles calculations are used to investigate the potassium ion (K^+) transport properties in K-hollandite. The calculated K^+ migration barrier energy is 0.44 eV at a pressure of 10 GPa, an energy quite small to block the K^+ migration in K-hollandite channels. The calculated ionic conductivity of K-hollandite is highly anisotropic and depends on its concentration of K^+ vacancies. About 6% K^+ vacancies in K-hollandite can lead to a higher conductivity compared to the conductivity of hydrated wadsleyite and ringwoodite in the mantle. K^+ vacancies being commonly found in many K-hollandite samples with maximum vacancies over 30%, the formation of K-hollandite during subduction of continental or alkali-rich oceanic crust can contribute to the high conductivity anomalies observed in subduction zones.

1. Introduction

K-hollandite ($KAlSi_3O_8$) is believed to form during the subduction process [*Ringwood et al.*, 1967; *Schmidt*, 1996; *Rapp et al.*, 2008; *Wu et al.*, 2009; *Ishii et al.*, 2012]. High temperature-pressure experiments confirm the existence of K-hollandite in hydrated average upper continental crust, mid-ocean ridge basalt (MORB), and andesite and pelitic rocks when pressure increases above 8 GPa [*Schmidt*, 1996; *Rapp et al.*, 2008; *Wu et al.*, 2009; *Ishii et al.*, 2012]. The stable temperature (T) and pressure (P) domain of K-hollandite ($1800\,K > T > 1000\,K$ and $128\,GPa > P > 8\,GPa$) suggests its stability in the upper and lower mantle [*Nishiyama et al.*, 2005].

The structure of K-hollandite is composed of four double chains of edge-shared SiO_6 or AlO_6 octahedra with a large enclosed square channel along the [001] axis (Figure 1a). Large-ion lithophile elements (LILEs), such as Rb, Ba, Sr, K, Pb, La, Ce, and Th, can be accommodated in the large channel and carried down into the deep mantle. The LILE enrichment of K-hollandite can explain the geochemical trace element abundance in oceanic island basalts [*Rapp et al.*, 2008]. The large channel structure can also provide a path for the migration of K^+. Materials sharing the hollandite structure are known as superionic conductors. Previous studies on hollandite-type $K_xTi_{1-y}Mn_yO_2$ (K-priderites), with 20% K^+ vacancies, show a very high K^+ conductivity of $20\,S\,m^{-1}$ at room temperature [*Khanna et al.*, 1981; *Yoshikado et al.*, 1982].

Previous calculations on K-hollandite investigated its equation of states, elasticity, and phase transition from a tetragonal (hollandite I) to a monoclinic phase (hollandite II) [*Mookherjee and Steinle-Neumann*, 2009; *Caracas and Ballaran*, 2010; *Mussi et al.*, 2010; *Deng et al.*, 2011; *Kawai and Tsuchiya*, 2013]. The latter revealed that K-hollandite exhibits strong shear wave anisotropy at high pressure, and [001] dislocations are favored under the shear stress of the subducted slabs [*Mussi et al.*, 2010]. This property might contribute significantly to the mantle seismic anisotropy prevailing in subduction zones [*Mookherjee and Steinle-Neumann*, 2009; *Caracas and Ballaran*, 2010; *Mussi et al.*, 2010; *Kawai and Tsuchiya*, 2013].

Beyond the seismic property, a thorough investigation of the transport properties of channel ions in K-hollandite should help better understand the variations in electrical conductivity of subduction zones and related recycling of LILEs. Here we present new calculations of the electrical conductivity of K-hollandite based on the climbing image nudged elastic band (CINEB) method and the First-Principles Molecular Dynamics (FPMD).

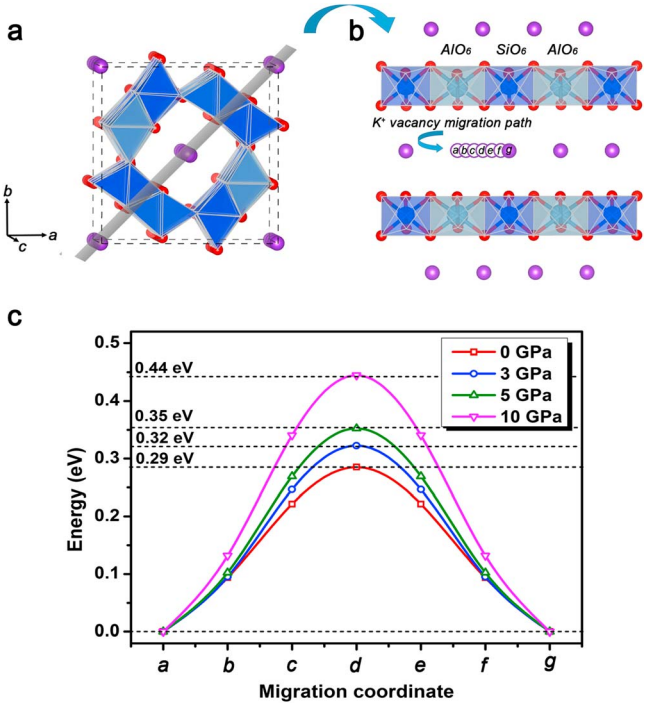

Figure 1. K^+ migration path and barrier energy in the crystal structure of Model A by CINEB simulation. (a) The crystal structure of K-hollandite. Deep purple, light blue, dark blue, and red spheres represent K, Al, Si, and O atoms, respectively. (b) $(\bar{1}10)$ slice cut from Figure 1a and the K^+ hopping by vacancy along the channel in K-hollandite, with the minimized energy migration path in the center of the channel from sites a to g. (c) Calculated energy barriers for K^+ migration along the path from sites a to g as shown in part Figure 1b at different pressures of 0 GPa, 3 GPa, 5 GPa, and 10 GPa, respectively.

2. Methods

The first-principles calculations were based on the density functional theory [*Hohenberg and Kohn*, 1965; *Kohn and Sham*, 1965] within the local density approximation [*Ceperley and Alder*, 1980; *Perdew and Zunger*, 1981]. All computations were carried out using the Vienna Ab Initio Simulation Package (VASP) [*Kresse and Furthmuller*, 1996]. The calculations include a plane wave representation of the wave function with a cutoff energy of 540 eV. The K ($3s^23p^64s^1$), Al ($3s^23p^1$), Si ($3s^23p^23d^0$), and O ($2s^22p^4$) orbits were treated as valence states.

To obtain minimum energy pathways and saddle points in K^+ migration, CINEB method was adopted [*Henkelman et al.*, 2000]. This method was used to calculate the barrier energy of H^+ migration in other mantle minerals [*Karki and Khanduja*, 2007; *Verma and Karki*, 2009]. For the investigation of high pressure-temperature (P-T) ionic conduction, the FPMD simulations were performed [*Mo et al.*, 2012; *Wang et al.*, 2015; *Kawai and Tsuchiya*, 2015]. In these calculations, a larger supercell $1 \times 1 \times 4$ containing 104 atoms was adopted. The supercell volume was derived from the calculated equation of state for K-hollandite, shown in Figure S2 in the supporting information, which is consistent with experimental results [*Zhang et al.*, 1993; *Nishiyama et al.*, 2005; *Ferroir et al.*, 2006]. The details of the simulations are given in Text S1.

In view of the disordered site occupation between Al and Si, two models with and without tetragonal symmetry were considered in our simulations. Model A (Figure 1a) applying the tetragonal symmetry was selected from the previous work of *Kawai and Tsuchiya* [2013] and Model B (Figure S1a) without tetragonal symmetry from the work of *Deng et al.* [2011].

3. Results and Discussion

Figure S2 illustrates the calculated Pressure-Volume-Temperature (P-V-T) relation used in calculating the K^+ migration barrier energy in K-hollandite at pressures of 0 GPa, 3 GPa, 5 GPa, and 10 GPa, respectively, and a temperature of 0 K. Due to a conspicuous one-dimensional (1-D) ion migration channel in K-hollandite, the interchannel K^+ migration was ignored in our calculation. For Model A, the migration of K^+ progresses along the center of the channel from sites *a* to *g* (Figure 1b). The barrier energy is 0.29 eV at 0 GPa but increases with applied pressure and reaches 0.44 eV at 10 GPa. The migration energy calculated for Model B is almost identical to that of Model A (Figure S1). Therefore, Model A is selected for the subsequent discussion.

To investigate the K^+ migration behavior at high P-T conditions, the FPMD simulations were carried out at a pressure of 10 GPa and various temperatures up to 1600 K. Figure 2 illustrates the mean square displacements (MSDs) of K^+ and the K^+ migration trajectories in the channel of the K-hollandite structure with different levels of K^+ vacancies at a pressure of 10 GPa and temperatures of 1000 K and 1600 K. Figure 2a clearly demonstrates an increase in MSDs correlated with the number of K^+ vacancies below a pressure of 10 GPa.

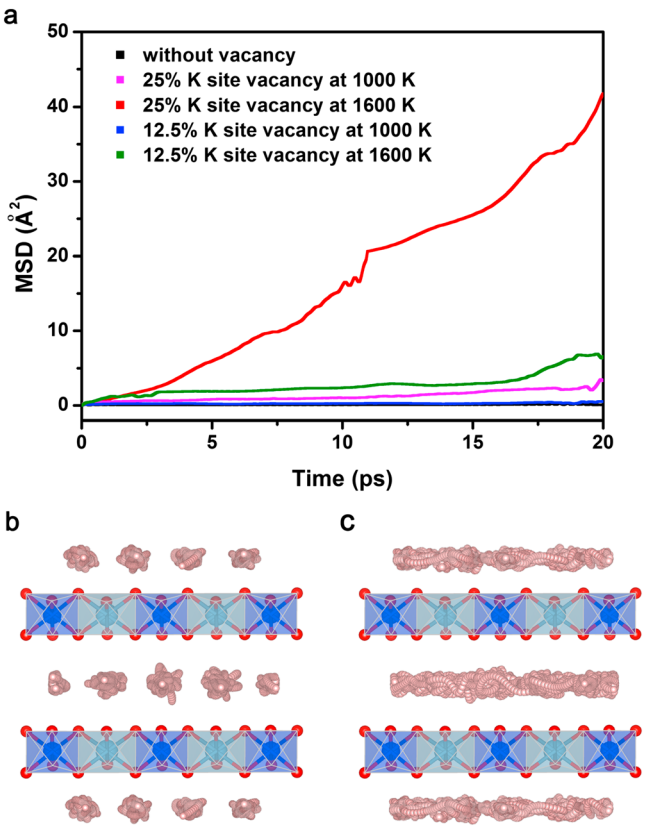

Figure 2. Comparison of K^+ migration behavior in the K-hollandite channel structure with and without a K^+ vacancy. (a) Calculated mean square displacements (MSDs) of K^+ without K^+ vacancy and with 12.5% and 25% K^+ vacancies at 1000 K and 1600 K under 10 GPa. (b, c) Trajectories (small pink bullets) of K^+ migration without K^+ vacancy and with 25% K^+ vacancies at 1600 K and 10 GPa for 20 ps viewed from the $(\bar{1}10)$ plane.

Figure 2b illustrates the K^+ migration trajectories confined to their equilibrium positions when the K^+ vacancy in K-hollandite structure is zero under 10 GPa and 1600 K. The migration trajectories were constantly extended along the channel of K-hollandite when the K^+ vacancies reached 25% (Figure 2c). The migration of K^+ in K-hollandite with 25% vacancies is also quite obvious even at 1000 K (Figure S3). Therefore, our results imply the migration of K^+ becoming substantially easier with an increasing number of K^+ vacancies in the K-hollandite structure. K^+ vacancies are commonly observed in several K-hollandite samples [*Domanik and Holloway*, 1996; *Wang and Takanashi*, 1999; *Domanik and Holloway*, 2000; *Langenhorst and Poirier*, 2000; *Rapp et al.*, 2008; *Wu et al.*, 2009; *Irifune et al.*, 2009; *Cid et al.*, 2014]. The non-stoichiometric molecular formulas of K-hollandite samples demonstrate a maximum of K^+ vacancy concentration up to 39%, with 2.63% coexisting oxygen vacancies (Table S1). The presence of K^+ vacancies was further discussed in Text S2.

A K-hollandite with 25% K^+ vacancies was employed to simulate the K^+ migration behavior at various temperatures under 10 GPa. The calculated K^+ diffusion coefficients from its MSDs were fitted through the Arrhenius equation at temperatures varying from 1000 K to 1600 K (Figure S4), from which a migration activation enthalpy of 0.63 eV was derived. Since a band gap over 5.0 eV (Figure S5) transforms the K-hollandite into an electronic insulator, K^+ conduction must play a dominant role in the mineral electrical conduction. Our simulation reveals the absence of Al, Si, or O diffusion up to 1600 K (Figure S6).

Considering the relative small number of Al, Si, and O vacancies and their indistinctive diffusion, we ignored their contribution to the total conductivity of K-hollandite. We can obtain the electrical conductivity of K-hollandite by applying the Nernst-Einstein equation (Text S1). The calculated electrical conductivity was plotted in Figure 3 revealing the conductivity of K-hollandite with 25% K^+ vacancies being $>20\,S\,m^{-1}$ at 1600 K and 10 GPa. K-hollandite can become a superionic conductor of K^+ with the K-hollandite channels not only storing K^+ but also creating a highway for the migration of K^+ at appropriate temperature and pressure conditions.

The high conductivity of K-hollandite predicted above could explain the observed high conductivity anomalies in subduction zones along the circum-Pacific margin [*Fukao et al.*, 2004; *Kelbert et al.*, 2009; *Shimizu et al.*, 2010]. The transition zone occurring beneath the northeastern China and the Philippine Sea especially displays a high *P* wave velocity and high conductivity reaching 0.5 to $2\,S\,m^{-1}$ [*Ichiki et al.*, 2001; *Fukao et al.*, 2004; *Kelbert et al.*, 2009; *Shimizu et al.*, 2010] that cannot be explained by proton conduction in the minerals wadsleyite or ringwoodite [*Fukao et al.*, 2004; *Huang et al.*, 2005; *Yoshino et al.*, 2008; *Dai and Karato*, 2009; *Guo and Yoshino*, 2013]. In Figure 3, we plotted the highest range of electrical conductivities ($0.5–2\,S\,m^{-1}$) from the subduction slabs transition zone lying beneath the Philippine Sea and northeastern China. Also reported are the electrical conductivities of wadsleyite and ringwoodite containing different water contents [*Huang et al.*, 2005;

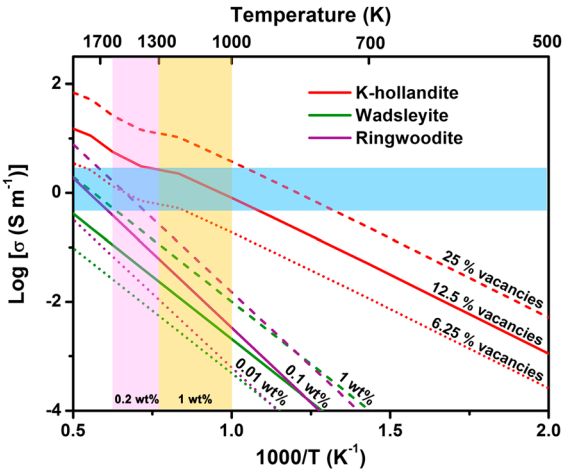

Figure 3. Comparison of the electrical conductivities of hydrous wadsleyite, hydrous ringwoodite, and K-hollandite with the electrical conductivity anomaly range of the transition zone in subducted slabs beneath the Philippine Sea and northeastern China. The electrical conductivities of wadsleyite and ringwoodite with different water contents [*Huang et al.*, 2005] are shown by the green and purple lines. Water contents of 0.01 wt %, 0.1 wt %, and 1 wt % are marked with dotted, solid, and dashed lines, respectively. The calculated K^+ conductivities of K-hollandite having 6.25%, 12.5%, and 25% of K^+ vacancies are shown with red dots and dashed and solid lines, respectively. The light blue area indicates the electrical conductivity anomaly range in the transition zone in subducted slabs beneath the Philippine Sea and northeastern China. The pink and yellow areas indicate the ranges in temperature prevailing in the slabs having water contents of 0.2 wt % and 1 wt % in the transition zone. The temperature ranges are cited from previous work [*Suetsugu et al.*, 2010; *Mao et al.*, 2012].

Dai and Karato, 2009] and the electrical conductivities of K-hollandite along the [001] direction having different levels of K^+ vacancies as a function of reciprocal temperature. Previous seismic investigations established on the basis of the geotemperature distribution within this transition zone (see the pink area in Figure 3) have shown a water content of only 0.2 wt % in wadsleyite or/and ringwoodite [*Green et al.*, 2010; *Suetsugu et al.*, 2010; *Mao et al.*, 2012]. Figure 3 also reveals that 1 wt % water content in ringwoodite is required to achieve a conductivity of 0.5–2 S m^{-1}, much higher than the 0.2 wt % water content expected in the transition zone. The water content requirement is $>$ 1 wt % for wadsleyite. Moreover, increasing the water content of the transition zone to 1 wt % generates a low temperature anomaly by 800 K (see the yellow area in Figure 3), that is, a "cold" transition zone is needed to fit the observed seismic velocity data [*Suetsugu et al.*, 2010; *Mao et al.*, 2012]. Unfortunately, within the temperature range of the cold transition zone, both the conductivities of wadsleyite and ringwoodite containing 1 wt % water will have decreased far below the electrical conductivity anomaly range (see Figure 3). Dense hydrous magnesium silicates also fail to explain the high conductivity of the transition zone [*Guo and Yoshino*, 2013]. The high seismic velocity suggests that partial melting and grain boundary fluid cannot be widely distributed and contribute to the high conductivity in this area. The high conductivity may be attributed to minerals formed in the mantel during subduction. Assuming K-hollandite with a [001] preferred orientation is widely present in the transition zone beneath the northeastern China and the Philippine Sea and considering the K^+ conductivity of K-hollandite creating the highest electrical conductivity anomaly, the above contradiction would be removed. About 6.25% of K^+ vacancies is enough for K-hollandite having the [001] preferred orientation to explain the electrical conductivity anomaly (Figure 3). The application of fast K^+ depends on whether K-hollandite with a favorable level of K^+ vacancies and with a [001] preferred orientation can occur in abundance in the transition zone of subducted slabs. Some evidence supporting this assertion can be summarized in the following: (1) Elevated K_2O concentrations in subducted slabs have been confirmed by chemical analyses of drill cores of oceanic crust from a series of drilling projects located at the front of the Ryukyu, Mariana, and Izu-Bonin trenches (Sites 292, 293, and 294; Ryukyu, Deep Sea Drilling Project, DSDP); from Site 801 (Mariana, Ocean Drilling Program, ODP); and from Site 1149 (Izu-Bonin, Ocean Drilling Program, ODP) [*Chen*, 1991]. The K_2O concentrations even reached 8.1 wt % in alkali basalts collected from Site 801 [*Kelley and Plank*, 2003]. Subducted slabs having such high K_2O contents could supply ample potassium to generate large amounts of K-hollandite during the subduction process. (2) High-P-T calculations and experiments have confirmed the existence of K-hollandite in the experimental products of hydrated average upper continental crust, MORB, andesite, and pelite undergoing pressure above 8 GPa [*Schmidt*, 1996; *Rapp et al.*, 2008; *Wu et al.*, 2009; *Ishii et al.*, 2012] and even into the lower mantle [*Nishiyama et al.*, 2005]. K-hollandite can form under pressure and temperature conditions prevailing in the transition zone during the subduction of oceanic slabs. (3) The Pacific plate becomes stagnant in the transition zone beneath northeastern China and the Philippine Sea [*Fukao et al.*, 2001]. This stagnation could provide

from the time and space point of view favorable conditions to the formation and accumulation of K-hollandite in the transition zone. It is also reported that the oceanic crustal layer can be folded and stored in the transition zone during subduction [*Yoshida and Tajima*, 2013]. This effect may also increase the content of K-hollandite in the transition zone so that both the electrical conductivity and seismic velocity anomalies can be resolved by seismic measurements and telluric electromagnetic sounding. The K^+ vacancy levels in K-hollandite under P-T conditions prevailing in the transition zone (see Text S2 and Table S1) may reach a level of 6.25%, which is enough to explain the electrical conductivity anomalies in the transition zone beneath northeastern China and the Philippine Sea. The [001] preferred orientation of K-hollandite in the Pacific transition zones is believed to exist based on the following assessments. First, a strong shear stress is acting on and is parallel to the downgoing subducted plate driven by mantle convection. This shear stress could generate the [001] fabric for the tetragonal cell parameters of K-hollandite that are strongly anisometric with [001] being much smaller than [100] or [010] [*Mussi et al*., 2010]. Second, the stagnant Pacific subducted plate in the transition zone beneath the northeastern China and the Philippine Sea [*Fukao et al*., 2001] could provide enough strain time for a complete transformation to the [001] fabric. Finally, the first-principles simulations [*Mookherjee and Steinle-Neumann*, 2009; *Caracas and Ballaran*, 2010; *Kawai and Tsuchiya*, 2013] have shown a strong shear wave anisotropy in the K-hollandite lattices with the preferred [001] direction being the fastest to propagate the seismic shear wave. Data processing of the higher mode Rayleigh and Love wave overtone revealed the existence of a seismic anisotropy in subduction slabs comprised in the transition zone (400–610 km) around the Pacific margin [*Trampert and Heijst*, 2002; *Visser et al*., 2008]. The vertically polarized shear wave velocity in these areas is faster than the horizontally polarized shear wave velocity [*Visser et al*., 2008]. The calculated anisotropy of shear wave propagation in K-hollandite being consistent with the field seismic wave velocity measurement, the K-hollandite [001] fabric might exist in subducted slabs comprised within the transition zones. In summary, the above evidence testifies to the existence of accumulated K-hollandite with preferred orientation [001] fabric, in subducted slabs comprised in the transition zone beneath the Philippine Sea and northeastern China. K-hollandite has a sufficient number of K^+ vacancies concentration to be using the [001] corridor for fast K^+ conduction mechanism and explain the high conductivity anomalies occurring in subduction zones along the circum-Pacific margin.

4. Conclusions

Through the first-principles calculations, we conclude that the K-hollandite mineral having a certain number of K^+ vacancies can transformed into a superionic conductor along its [001] lattice direction under pressure and temperature conditions prevailing in the deep mantle. This discovery can provide a good explanation for the high conductivity anomalies which occur in subduction zones along the circum-Pacific margin, especially in the transition zone beneath northeastern China and the Philippine Sea. It is, however, difficult to justify the anomaly by the proton conduction mechanism of hydrated wadsleyite and ringwoodite because it is incompatible with the seismic wave velocity measurements. Performing future integrated inversions of deep electrical conductivity and on seismic wave velocity profiles would render possible the analysis of the specific distribution of K-hollandite in deep subducted slabs. This will further help understand the recycling of incompatible elements in the deep mantle and the origin of the incompatible elements-enriched basalts.

Acknowledgments

We thank two anonymous reviewers for their careful reading and valuable comments, which helped to improve the manuscript. This study was supported by the Strategic Priority Research Program (B) of the Chinese Academy of Sciences (XDB18010401), NSFC (51302259), and "135" Program of Institute of Geochemistry, CAS. We are grateful to X. J. Huang, W. G. Zhou, and Y. G. Liu for discussions.

References

Caracas, R., and T. B. Ballaran (2010), Elasticity of (K, Na)$AlSi_3O_8$ hollandite from lattice dynamics calculations, *Phys. Earth Planet. Inter.*, *181*, 21–26.

Ceperley, D., and B. Alder (1980), Ground state of the electron gas by a stochastic method, *Phys. Rev. Lett.*, *45*, 566–569.

Chen, J. (1991), Geochemical studies of basalts from the Philippine Sea, *J. Southeast Asian Earth Sci.*, *6*, 63–68.

Cid, J. P., L. V. S. Nardi, C. P. Cid, P. E. Gisbert, and N. M. Balzaretti (2014), Acid compositions in a veined-lower mantle, as indicated by inclusions of (K, Na)-hollandite + SiO_2 in diamonds, *Lithos*, *196-197*, 42–53.

Dai, L., and S. Karato (2009), Electrical conductivity of wadsleyite at high temperatures and high pressures, *Earth Planet. Sci. Lett.*, *287*, 277–283.

Deng, L., X. Liu, H. Liu, and Y. Zhang (2011), A first-principles study of the phase transition from Holl-I to Holl-II in the composition $KAlSi_3O_8$, *Am. Mineral.*, *96*, 974–982.

Domanik, K. J., and J. R. Holloway (1996), The stability and composition of phengitic muscovite and associated phases from 5.5 to 11 GPa: Implications for deeply subducted sediments, *Geochim. Cosmochim. Acta*, *60*, 4133–4150.

Domanik, K. J., and J. R. Holloway (2000), Experimental synthesis and phase relations of phengitic muscovite from 6.5 to 11 GPa in a calcareous metapelite from the Dabie Mountains, China, *Lithos*, *52*, 51–77.

Ferroir, T., T. Onozawa, T. Yagi, S. Merkel, N. Miyajima, N. Nishiyama, T. Irifune, and T. Kikegawa (2006), Equation of state and phase transition in $KAlSi_3O_8$ hollandite at high pressure, *Am. Mineral.*, *91*, 327–332.

Fukao, Y., S. Widiyantoro, and M. Obayashi (2001), Stagnant slabs in the upper and lower mantle transition region, *Rev. Geophys.*, *39*, 291–323, doi:10.1029/1999RG000068.
Fukao, Y., T. Koyama, M. Obayashi, and H. Utada (2004), Trans-Pacific temperature field in the mantle transition region derived from seismic and electromagnetic tomography, *Earth Planet. Sci. Lett.*, *217*, 425–434.
Green, H. W., II, W.-P. Chen, and M. R. Brudzinski (2010), Seismic evidence of negligible water carried below 400 km depth in subducting lithosphere, *Nature*, *467*, 828–831.
Guo, X., and T. Yoshino (2013), Electrical conductivity of dense hydrous magnesium silicates with implication for conductivity in the stagnant slab, *Earth Planet. Sci. Lett.*, *369-370*, 239–247.
Henkelman, G., B. P. Uberuaga, and H. Jonsson (2000), A climbing image nudged elastic band method for finding saddle points and minimum energy paths, *J. Chem. Phys.*, *113*, 9901–9904.
Hohenberg, P., and W. Kohn (1965), Inhomogeneous electron gas, *Phys. Rev. B*, *136*, 864–871.
Huang, X., Y. Xu, and S. –. I. Karato (2005), Water content in the transition zone from electrical conductivity of wadsleyite and ringwoodite, *Nature*, *434*, 746–749.
Ichiki, M., M. Uyeshima, H. Utada, Z. Guoze, T. Ji, and M. Mingzhi (2001), Upper mantle conductivity structure of the back-arc region beneath northeastern China, *Geophys. Res. Lett.*, *28*, 3773–3776, doi:10.1029/2001GL012983.
Irifune, T., A. E. Ringwood, and W. O. Hibberson (2009), Subduction of continental crust and terrigenous and pelagic sediments: An experimental study, *Earth Planet. Sci. Lett.*, *126*, 351–368.
Ishii, T., H. Kojitani, and M. Akaogi (2012), High-pressure phase transitions and subduction behavior of continental crust at pressure–temperature conditions up to the upper part of the lower mantle, *Earth Planet. Sci. Lett.*, *357–358*, 31–41.
Karki, B. B., and G. Khanduja (2007), A computational study of ionic vacancies and diffusion in $MgSiO_3$ perovskite and post-perovskite, *Earth Planet. Sci. Lett.*, *260*, 201–211.
Kawai, K., and T. Tsuchiya (2013), First-principles study on the high-pressure phase transition and elasticity of $KAlSi_3O_8$ hollandite, *Am. Mineral.*, *98*, 207–218.
Kawai, K., and T. Tsuchiya (2015), Small shear modulus of cubic $CaSiO_3$ perovskite, *Geophys. Res. Lett.*, *42*, 2718–2726, doi:10.1002/2015GL063446.
Kelbert, A., A. Schultz, and G. Egbert (2009), Global electromagnetic induction constraints on transition-zone water content variations, *Nature*, *460*, 1003–1006.
Kelley, K. A., and T. Plank (2003), Composition of altered oceanic crust at ODP Sites 801 and 1149, *Geochem. Geophys. Geosyst.*, *4*(6), 8910, doi:10.1029/2002GC000435.
Khanna, S. K., G. Gruner, R. Orbach, and H. U. Beyeler (1981), Thermally activated microwave conductivity in the superionic conductor hollandite ($K_{1.54}Mg_{0.77}Ti_{7.23}O_{16}$), *Phys. Rev. Lett.*, *47*, 255–257.
Kohn, W., and L. J. Sham (1965), Self-consistent equations including exchange and correlation effects, *Phys. Rev. A*, *140*, 1133–1138.
Kresse, G., and J. Furthmüller (1996), Efficient iterative schemes for ab initio total-energy calculations using a plane-wave basis set, *Phys. Rev. B*, *54*, 11,169–11,186.
Langenhorst, F., and J.-P. Poirier (2000), 'Eclogitic' minerals in a shocked basaltic meteorite, *Earth Planet. Sci. Lett.*, *176*, 259–265.
Mao, Z., J. –. F. Lin, S. D. Jacobsen, T. S. Duffy, Y. –. Y. Chang, J. R. Smyth, D. J. Frost, E. H. Hauri, and V. B. Prakapenka (2012), Sound velocities of hydrous ringwoodite to 16 GPa and 673 K, *Earth Planet. Sci. Lett.*, *331–332*, 112–119.
Mo, Y., S. P. Ong, and G. Ceder (2012), First principles study of the $Li_{10}GeP_2S_{12}$ lithium super ionic conductor material, *Chem. Mater.*, *24*, 15–17.
Mookherjee, M., and G. Steinle-Neumann (2009), Detecting deeply subducted crust from the elasticity of hollandite, *Earth Planet. Sci. Lett.*, *288*, 349–358.
Mussi, A., P. Cordier, D. Mainprice, and D. J. Frost (2010), Transmission electron microscopy characterization of dislocations and slip systems in K-lingunite: Implications for the seismic anisotropy of subducted crust, *Phys. Earth Planet. Inter.*, *182*, 50–58.
Nishiyama, N., R. P. Rapp, T. Irifune, T. Sanehira, D. Yamazaki, and K. Funakoshi (2005), Stability and P–V–T equation of state of $KAlSi_3O_8$-hollandite determined by in situ X-ray observations and implications for dynamics of subducted continental crust material, *Phys. Chem. Miner.*, *32*, 627–637.
Perdew, J. P., and A. Zunger (1981), Self-interaction correction to density functional approximations for many-electron systems, *Phys. Rev. B*, *23*, 5048–5079.
Rapp, R. P., T. Irifune, S. Nobu, N. Nishiyama, M. D. Norman, and T. Inoue (2008), Subduction recycling of continental sediments and the origin of geochemically enriched reservoirs in the deep mantle, *Earth Planet. Sci. Lett.*, *271*, 14–23.
Ringwood, A. E., A. F. Fredi, and A. D. Wadsley (1967), High-pressure $KAlSi_3O_8$ and aluminosilicate with sixfold coordination, *Acta Crystallogr.*, *23*, 1093–1095.
Schmidt, M. W. (1996), Experimental constraints on recycling of potassium from subducted oceanic crust, *Science*, *272*, 1927–1930.
Shimizu, H., H. Utada, K. Baba, T. Koyama, M. Obayashi, and Y. Fukao (2010), Three-dimensional imaging of electrical conductivity in the mantle transition zone beneath the North Pacific Ocean by a semi-global induction study, *Phys. Earth Planet. Inter.*, *183*, 252–269.
Suetsugu, D., et al. (2010), Depths of the 410 km and 660 km discontinuities in and around the stagnant slab beneath the Philippine Sea: Is water stored in the stagnant slab?, *Phys. Earth Planet. Inter.*, *183*, 270–279.
Trampert, J., and H. J. Heijst (2002), Global azimuthal anisotropy in the transition zone, *Science*, *296*, 1297–1299.
Verma, A. K., and B. B. Karki (2009), Ab initio investigations of native and protonic point defects in Mg_2SiO_4 polymorphs under high pressure, *Earth Planet. Sci. Lett.*, *285*, 140–149.
Visser, K., J. Trampert, S. Lebedev, and B. L. N. Kennett (2008), Probability of radial anisotropy in the deep mantle, *Earth Planet. Sci. Lett.*, *270*, 241–250.
Wang, W., and E. Takanashi (1999), Subsolidus and melting experiments of a K-rich basaltic composition to 27 GPa: Implication for the behavior of potassium in the mantle, *Am. Mineral.*, *84*, 357–361.
Wang, Y., W. D. Richards, S. P. Ong, L. J. Miara, J. C. Kim, Y. F. Mo, and G. Ceder (2015), Design principles for solid-state lithium superionic conductors, *Nat. Mater.*, *14*, 1026–1031.
Wu, Y., Y. Fei, Z. Jin, and X. Liu (2009), The fate of subducted upper continental crust: An experimental study, *Earth Planet. Sci. Lett.*, *282*, 275–284.
Yoshida, M., and F. Tajima (2013), On the possibility of a folded crustal layer stored in the hydrous mantle transition zone, *Phys. Earth Planet. Inter.*, *219*, 34–48.
Yoshikado, S., T. Ohachi, I. Taniguchi, Y. Onoda, M. Watanabe, and Y. Fujiki (1982), Ionic conductivity of hollandite type compounds from 100 Hz to 37.0 GHz, *Solid State Ionics*, *7*, 335–344.
Yoshino, T., G. Manthilake, T. Matsuzaki, and T. Katsura (2008), Dry mantle transition zone inferred from the conductivity of wadsleyite and ringwoodite, *Earth Planet. Sci. Lett.*, *287*, 277–283.
Zhang, J., J. Ko, R. M. Hazen, and G. T. Prewitt (1993), High-pressure crystal chemistry of $KAlSi_3O_8$ hollandite, *Am. Mineral.*, *78*, 493–499.